

2021

Brain volumetric deficits in MAPT mutation carriers: A multisite study

Stephanie A. Chu
University of California, San Francisco

Nupur Ghoshal
Washington University School of Medicine in St. Louis

et al

Follow this and additional works at: https://digitalcommons.wustl.edu/open_access_pubs





Recommended Citation

Chu, Stephanie A.; Ghoshal, Nupur; and et al, "Brain volumetric deficits in MAPT mutation carriers: A multisite study." *Annals of Clinical and Translational Neurology*. 8,1. . (2021).
https://digitalcommons.wustl.edu/open_access_pubs/10309

This Open Access Publication is brought to you for free and open access by Digital Commons@Becker. It has been accepted for inclusion in Open Access Publications by an authorized administrator of Digital Commons@Becker. For more information, please contact vanam@wustl.edu.

RESEARCH ARTICLE

Brain volumetric deficits in *MAPT* mutation carriers: a multisite study

Stephanie A. Chu¹ , Taru M. Flagan¹, Adam M. Staffaroni¹, Lize C. Jiskoot^{2,3}, Jersey Deng¹, Salvatore Spina¹, Liwen Zhang¹, Virginia E. Sturm¹, Jennifer S. Yokoyama¹, William W. Seeley¹, Janne M. Papma², Dan H. Geschwind⁴, Howard J. Rosen¹, Bradley F. Boeve⁵, Adam L. Boxer¹, Hilary W. Heuer¹, Leah K. Forsberg⁵, Danielle E. Brushaber⁵, Murray Grossman⁶, Giovanni Coppola⁴, Bradford C. Dickerson⁷, Yvette M. Bordelon⁴, Kelley Faber⁸, Howard H. Feldman⁹, Julie A. Fields⁵, Jamie C. Fong¹, Tatiana Foroud⁸, Ralitza H. Gavrilova⁵, Nupur Ghoshal¹⁰, Neill R. Graff-Radford¹¹, Ging-Yuek Robin Hsiung¹², Edward D. Huey¹³, David J. Irwin⁴, Kejal Kantarci⁶ , Daniel I. Kaufer¹⁴, Anna M. Karydas¹, David S. Knopman⁵ , John Kornak¹⁵, Joel H. Kramer¹, Walter A. Kukull¹⁶, Maria I. Lapid⁵, Irene Litvan⁹, Ian R.A. Mackenzie¹², Mario F. Mendez⁴, Bruce L. Miller¹, Chiadi U. Onyike¹⁷, Alexander Y. Pantelyat¹⁷, Rosa Rademakers¹¹, Eliana Marisa Ramos⁴, Erik D. Roberson¹⁸, Maria Carmela Tartaglia¹⁹, Nadine A. Tatton²⁰, Arthur W. Toga²¹, Ashley Vetor⁸, Sandra Weintraub²², Bonnie Wong⁷, Zbigniew K. Wszolek¹¹, the ARTFL/LEFFTDS Consortium, John C. Van Swieten² & Suzee E. Lee¹ 

¹Memory and Aging Center, Department of Neurology, Weill Institute for Neurosciences, University of California, San Francisco, San Francisco, California

²Erasmus Medical Center, Rotterdam, Netherlands

³Dementia Research Center, University College London, London, UK

⁴University of California, Los Angeles, Los Angeles, California

⁵Mayo Clinic, Rochester, Minnesota

⁶Perelman School of Medicine, University of Pennsylvania, Philadelphia, Pennsylvania

⁷Massachusetts General Hospital, Boston, Massachusetts

⁸School of Medicine, Indiana University, Indianapolis, Indiana

⁹University of California, San Diego, La Jolla, California

¹⁰Washington University School of Medicine, St. Louis, Missouri

¹¹Mayo Clinic, Jacksonville, Florida

¹²University of British Columbia, Vancouver, British Columbia, Canada

¹³Departments of Psychiatry and Neurology, Columbia University, New York, New York

¹⁴University of North Carolina, Chapel Hill, North Carolina, USA

¹⁵Department of Epidemiology and Biostatistics, University of California, San Francisco, San Francisco, California

¹⁶National Alzheimer's Coordinating Center, University of Washington, Seattle, Washington

¹⁷Johns Hopkins University School of Medicine, Baltimore, Maryland

¹⁸University of Alabama at Birmingham, Birmingham, Alabama

¹⁹Tanz Centre for Research in Neurodegenerative Diseases, University of Toronto, Toronto, Ontario, Canada

²⁰The Association for Frontotemporal Degeneration, Radnor, Pennsylvania

²¹USC Mark and Mary Stevens Neuroimaging and Informatics Institute, University of Southern California, Los Angeles, California

²²Northwestern Feinberg School of Medicine, Chicago, Illinois

Funding information

This work was supported by the Tau Consortium (SEL, GC, DHG, NG); National Institutes of Health [SEL: K23AG039414, R01 AG058233; GC: P50 AG023501, P01 AG019724, U54 NS092089; DHG: AG035610, R01 AG26938; RR: R35 NS097261, UG3 NS103870; EDH: R01 NS076837; BFB: U01 AG045390; ALB: U54NS092089, 2R01AG038791; HJR: U01 AG045390, U54 NS092089, K24 AG045333, R01 AG032306; BLM: P01AG019724, P50AG23501; AWT: P41EB015922; WWS: AG023501, AG19724; NG: K12 HD001459; JSY: K01 AG049152; SS: K08 AG052648; DJI: K23NS088341; MG: P01AG017586, U01AG052943; IL: 5P50AG005131-33, 2R01AG038791-06A, U01NS090259, 1U54 NS 092089, U01NS100610, U01NS80818, R25NS098999, P20GM109025; JK: R01EB022055, U01AG045390, U54NS092089, R01CA132870]; the John Douglas French Alzheimer's Foundation [GC, DHG]. Samples from the National Cell Repository for Alzheimer's Disease and Related Dementias (NCRAD), which receives government support under a cooperative agreement grant (U24AG21886) awarded by the National Institute on Aging (NIA), were used in this study. Data collection and dissemination of the data presented in this manuscript were supported by the LEFFTDS & ARTFL Consortium (LEFFTDS: U01 AG045390, funded by the National Institute on Aging and the National Institute of Neurological Diseases and Stroke; ARTFL: U54 NS092089, funded by the National Institute of Neurological Diseases and Stroke and National Center for Advancing Translational Sciences). ZKW is partially supported by the Mayo Clinic Center for Regenerative Medicine, the gifts from The Sol Goldman Charitable Trust, and the Donald G. and Jodi P. Heeringa Family, by the Haworth Family Professorship in Neurodegenerative Diseases fund, and by the Albertson Parkinson's Research Foundation. IRAM is supported by the Canadian Institutes of Health Research (74580). JCVS is supported by the Dioraphte Foundation grant (09-02-00), the Association for Frontotemporal Dementias Research Grant 2009, The Netherlands Organization for Scientific Research (NWO) grant (HCMI 056-13-018), and ZonMw Memorabel (project number 733050813). The Dutch cohort is

supported by ZonMw Memorabel (733050103 & 733050813), Alzheimer Nederland, JPND PreFrontAls consortium, and Bluefield Project. IL is additionally supported by the Parkinson Study Group, Michael J. Fox Foundation, Lewy Body Association, AVID Pharmaceuticals, Abbvie, Biogen and Roche.

Correspondence

Suzee Lee, Memory and Aging Center, Department of Neurology, University of California, San Francisco, San Francisco, California, USA. Tel: 415-514-3572; Fax: 415-353-8292; E-mail: Suzee.Lee@ucsf.edu

Received: 3 September 2020; Accepted: 18 October 2020

Annals of Clinical and Translational Neurology 2021; 8(1): 95–110

doi: 10.1002/acn3.51249

Abstract

Objective: *MAPT* mutations typically cause behavioral variant frontotemporal dementia with or without parkinsonism. Previous studies have shown that symptomatic *MAPT* mutation carriers have frontotemporal atrophy, yet studies have shown mixed results as to whether presymptomatic carriers have low gray matter volumes. To elucidate whether presymptomatic carriers have lower structural brain volumes within regions atrophied during the symptomatic phase, we studied a large cohort of *MAPT* mutation carriers using a voxelwise approach. **Methods:** We studied 22 symptomatic carriers (age 54.7 ± 9.1 , 13 female) and 43 presymptomatic carriers (age 39.2 ± 10.4 , 21 female). Symptomatic carriers' clinical syndromes included: behavioral variant frontotemporal dementia (18), an amnesic dementia syndrome (2), Parkinson's disease (1), and mild cognitive impairment (1). We performed voxel-based morphometry on T1 images and assessed brain volumetrics by clinical subgroup, age, and mutation subtype. **Results:** Symptomatic carriers showed gray matter atrophy in bilateral frontotemporal cortex, insula, and striatum, and white matter atrophy in bilateral corpus callosum and uncinate fasciculus. Approximately 20% of presymptomatic carriers had low gray matter volumes in bilateral hippocampus, amygdala, and lateral temporal cortex. Within these regions, low gray matter volumes emerged in a subset of presymptomatic carriers as early as their thirties. Low white matter volumes arose infrequently among presymptomatic carriers. **Interpretation:** A subset of presymptomatic *MAPT* mutation carriers showed low volumes in mesial temporal lobe, the region ubiquitously atrophied in all symptomatic carriers. With each decade of age, an increasing percentage of presymptomatic carriers showed low mesial temporal volume, suggestive of early neurodegeneration.

Introduction

Mutations in the microtubule-associated protein tau (*MAPT*) cause behavioral variant frontotemporal dementia (bvFTD) with or without parkinsonism, with some patients meeting criteria for progressive supranuclear palsy (PSP) or corticobasal syndrome.¹ As in sporadic bvFTD, in bvFTD due to *MAPT* mutations (bvFTD-*MAPT*), patients show degeneration in the anterior cingulate cortex, insula, striatum, and the amygdala.^{2,3} In contrast to sporadic bvFTD, however, bvFTD-*MAPT* more prominently targets the mesial temporal lobe and in particular, the hippocampus, a region less typically atrophied in sporadic bvFTD.^{2,3}

Less is known about the timing of brain volume changes during the presymptomatic phase. Early studies with small samples suggested that presymptomatic *MAPT* mutation carriers did not have apparent gray or white matter volume differences compared to controls.^{4,5} Studies with larger samples, however, have shown mixed results. A study of 26 symptomatic and presymptomatic

MAPT mutation carriers revealed gray matter trajectories that suggested that low hippocampus and amygdala volumes arise years before expected symptom onset.⁶ A diffusion tensor imaging study of 30 presymptomatic *MAPT* mutation carriers found early loss of white matter integrity.⁷ In contrast, a study of 23 presymptomatic *MAPT* mutation carriers did not show significantly low gray matter volumes, although there was a trend toward small regions of low gray matter volume in mesial temporal lobes.⁸

Most previous studies of presymptomatic *MAPT* mutation carriers have reported only group comparisons whose limitation is that they do not account for individual anatomical variation, which could account for mixed results across studies. To address this gap, we studied a multisite cohort of 65 *MAPT* mutation carriers (22 symptomatic and 43 presymptomatic) by analyzing structural MRI scans with a voxelwise method that detects gray and white matter differences in individual carriers. We hypothesized that: 1) regions of low gray or white matter volume in presymptomatic *MAPT* mutation carriers

would resemble atrophy patterns seen in symptomatic carriers, and 2) a subset of the presymptomatic carriers, that is, those presumably closer to symptom onset, would harbor low gray and white matter volumes beyond expected of their age. Previous literature suggests that specific *MAPT* mutations manifest different clinical syndromes;¹ therefore, we also explored whether different *MAPT* mutation subtypes targeted distinct neuroanatomical regions.

Methods

Participants

Study participants were recruited from: the Memory and Aging Center at the University of California, San Francisco (UCSF); Erasmus University Rotterdam; and two multisite genetic FTD research projects, the Advancing Research and Treatment for Frontotemporal Lobar Degeneration (ARTFL) and Longitudinal Evaluation of Familial Frontotemporal Dementia Subjects (LEFFTDS) (Table S1). Clinical diagnoses were rendered by the respective study sites.⁹

We studied 22 symptomatic *MAPT* mutation carriers, 43 presymptomatic *MAPT* mutation carriers and 107 healthy controls, comprised of 91 noncarrier genetic frontotemporal lobar degeneration family members and 16 unrelated controls (Table 1). These unrelated controls were added to the noncarrier family members to create an even distribution of ages that was similar to the age range of the *MAPT* mutation carrier cohorts. Among the 22 symptomatic carriers, 18 had a clinical diagnosis of bvFTD. Of the 18 with bvFTD, six carried secondary diagnoses, including PSP syndrome (4); parkinsonism (1); and depression (1). Of the four remaining symptomatic carriers: two had an amnesic dementia syndrome, one of which also had mild behavioral symptoms; one had Parkinson's disease (PD) with behavioral symptoms not meeting bvFTD criteria; and one had mild cognitive

impairment with behavior and language symptoms. All symptomatic carriers were recruited from UCSF, ARTFL, or LEFFTDS (Erasmus University did not recruit symptomatic patients).

Presymptomatic carriers were diagnosed as clinically normal by each respective study site. These participants were required to have a Mini-Mental State Examination (MMSE) score ≥ 27 , and if the participant did not have an MMSE score available, participants had a Montreal Cognitive Assessment (MoCA)¹⁰ score ≥ 21 . We chose this threshold for the MoCA score because in participants tested with both measures, an MMSE score of 27 corresponds to a MoCA score of 21.¹¹ We included three presymptomatic carriers with a Clinical Dementia Rating Scale (CDR®) plus Behavioral and Language Domains from the National Alzheimer's Coordinating Center (NACC) FTLT module (CDR® plus NACC FTLT)¹² global score of 0.5, as this score may not necessarily be indicative of incipient phenoconversion to disease. Nevertheless, we repeated each analysis without the three presymptomatic carriers who had a CDR® plus NACC FTLT global score of 0.5.

Healthy controls were also required to have a MMSE score ≥ 27 or a MoCA score ≥ 21 , a CDR® plus NACC FTLT global score of 0, and no significant history of neurological disease. All participants in the study were required to have a MRI brain scan free of structural lesions and prominent white matter disease.

Participants underwent neuropsychological tests at each site.^{4,13,14} The CDR® plus NACC FTLT scale was available for the UCSF and ARTFL/LEFFTDS cohorts. Neuropsychological tests were administered within 90 days of a participant's MRI scan. We calculated z-scores for each measure for each participant based on scores of the healthy controls. For variables with skewed distributions, we reflected and log transformed the data to improve the normality of the distribution prior to fitting multiple regression models. Because these z-scores were not adjusted for demographic characteristics, we compared

Table 1. Demographics of presymptomatic and symptomatic *MAPT* mutation carriers.

	Presymptomatic	Symptomatic	Healthy Controls
<i>n</i>	43	22	107
Age at MRI scan, years	39.2 (10.4)	54.7 (9.1)	48.9 (13.2)
M:F, <i>n</i>	22:21	9:13	51:56
Education, years	16.1 (2.4)	15.1 (2.4)	15.9 (2.3)
Education, Dutch 7-point scale ¹	4.8 (1.7)	n/a	5.3 (1.1)
Age at symptom onset	n/a	45.6 (8.3)	n/a
CDR® plus NACC FTLT, global score (0-3)	0.05 (0.15)	1.75 (0.98)	0 (0)
CDR® plus NACC FTLT, sum of boxes (max = 24)	0.07 (0.22)	9.73 (6.13)	0 (0)

Unless otherwise indicated, mean values are reported followed by the standard deviation in parentheses.

¹Erasmus participants were categorized into levels from 1 = less than 6 years of education to 7 = completed a university degree.

the z-scores of these cognitive measures for the presymptomatic, symptomatic, and control groups using multiple regression with age, education, and sex as covariates of no interest. We compared each *MAPT* mutation carrier group to controls using post hoc group-wise comparisons.

The Institutional Review Boards at each site approved this study, and participants or their surrogates provided informed consent to participate.

Genetic analysis

Participants were screened for pathogenic *MAPT* mutations.¹⁵ All *MAPT* mutation carriers in the study also tested negative for *GRN* mutations and for the *C9orf72* repeat expansion.

Image acquisition and preprocessing

Each participant underwent a T1-weighted structural MRI scan on a 3T scanner. Participants from UCSF were scanned on a Siemens Tim Trio or a Siemens Prisma scanner (Table S1). All T1-weighted images were preprocessed with SPM12 (<https://www.fil.ion.ucl.ac.uk/spm/>). T1-weighted images were preprocessed using standard spatial normalization in the SPM12 segment module, using the six standard tissue probability maps with a light clean up. Standard affine regularization with the International Consortium for Brain Mapping European brain template and warping regularization with the default parameters were used. Images were then segmented into gray and white matter images, which were smoothed using an 8-mm full width at half maximum isotropic Gaussian kernel.

Gray and white matter w-score maps

For each *MAPT* mutation carrier, we created gray matter and white matter w-score maps (w-maps) which represent the difference between the participant's actual gray or white matter values in each voxel and the expected value based on a group of healthy controls.¹⁶ A map of w-scores can be conceptualized as a z-score map of the gray or white matter residuals after adjustment for covariates of no interest via regression. To calculate a w-score, voxelwise linear regressions were performed on healthy control gray and white matter maps to determine the standard deviation of the residuals. Next, the w-score for each individual participant was calculated voxelwise using the following formula: $w = [(participant's\ value - value\ predicted\ for\ participant\ age) / SD\ of\ residuals\ of\ the\ healthy\ control\ group]$. Covariates of no interest included age, sex, total intracranial volume, site, scanner model,

and scan acquisition protocol. Since the w-score control group is utilized to build a reference range for brain volume, we selected controls to cover the age distribution of the mutation carriers. We prioritized selecting 91 available mutation-negative family members for our control group and also included 16 unrelated healthy controls because of the importance of an even age distribution in our models.

Gray and white matter relationships with age or symptom severity

We created group mean w-maps for 1) presymptomatic and 2) symptomatic carriers by averaging participants' w-scores voxelwise and thresholded the maps at $w \leq -2$.^{16,17} To create frequency gray and white matter w-maps, we determined the percentage of participants with gray or white matter values of $w \leq -2$ voxelwise. For presymptomatic carriers, we created group frequency w-maps binned by age (in decades) to visualize gray and white matter relationships with age. For symptomatic carriers, group frequency w-maps were binned by symptom severity, defined by the CDR® plus NACC FTLD global score.

Hemispheric symmetry analysis

Previous studies suggest bilateral and symmetric involvement in symptomatic *MAPT* mutation carriers.^{2,3,6} To determine whether atrophy or low brain volume in symptomatic and presymptomatic *MAPT* mutation carriers is symmetric at an individual-subject level, we calculated the difference between each participant's mean left and right hemisphere w-scores for gray or white matter.

Correlations between memory measures and hippocampal volume

We performed two analyses to explore associations between memory measures and the volume of the hippocampus, selected as an *a priori* region because of its importance in memory recall. First, we calculated for each participant the mean gray matter w-scores for the left and right hippocampi (defined by the Automated Anatomical Labeling atlas¹⁸). Verbal memory z-scores were based on either the California Verbal Learning Test II (CVLT-II) 10 minute delayed recall (UCSF; ARTFL/LEFFTDS) or the Rey Auditory Verbal Learning Test delayed recall trials (Erasmus). Spatial memory z-scores were based on the Benson figure recall (UCSF; ARTFL/LEFFTDS). We performed Spearman's correlations between participants' hippocampal w-scores and memory z-scores. Second, we selected the voxel most frequently showing reduced gray matter across all carriers and created a 4-mm sphere

around that voxel (and its contralateral homolog) to determine whether gray matter volume in this *MAPT*-targeted region correlates with verbal and visual memory measures. For these analyses, we correlated left hippocampus w-scores with verbal memory scores and right hippocampus w-scores with spatial memory z-scores given the importance of the left hippocampus for verbal memory¹⁹ and the right hippocampus for spatial memory.²⁰ Next, we searched voxelwise to identify brain regions where lower memory performance was associated with lower gray matter volume by correlating verbal then spatial memory z-scores with gray matter w-maps thresholded at $P < 0.05$ corrected for family-wise error.

The above correlations were performed in all carriers combined, symptomatic carriers, and presymptomatic carriers.

***MAPT* mutation subgroup analysis**

Our cohort consisted of participants carrying 13 different *MAPT* mutations. Because some mutations had low numbers of participants, we examined *MAPT* mutation subtypes categorized into five groups by either clinical (bvFTD-type; amnesic-type; PSP/PD-type) or neuropathological (four repeat-type (4R); and Pick bodies type) similarity to explore whether different types of *MAPT* mutations may target distinct neuroanatomy. The bvFTD group was comprised of carriers with the V337M mutation, a missense mutation located on exon 12 which typically causes bvFTD.²¹ The amnesic-type group consisted of carriers with R406W, a missense mutation on exon 13 which typically manifests with an amnesic syndrome reminiscent of an Alzheimer's-like syndrome rather than a bvFTD syndrome.^{22,23} The PSP/PD-type group consisted of carriers with mutations in N279K, S305N, and S305S, all exon 10 missense mutations which increase the ratio of 4R to three repeat (3R) tau; these mutations most often cause bvFTD with PSP or parkinsonism.^{24–28} The 4R-type group consisted of P301L, S305I, IVS10 + 16C>T, and IVS9-10G> T, a combination of exonic and splicing mutations which typically present with bvFTD; these mutations increase exon 10 transcription, which increases the ratio of 4R to 3R tau.^{15,29,30} The fifth group was the Pick bodies type group which contained G389R, G272V, S320F, and L315R mutations, all characterized by the inclusion of Pick body or Pick body-like pathology.^{31–34} Each group consisted of fewer than 10 symptomatic and presymptomatic carriers combined, with the exception of the 4R-type group, which had 31 carriers. To protect participant anonymity, we chose not to report the specific number within each group. We created mean w-maps for these five mutation subgroups to assess whether different mutation subtypes target distinct

anatomical regions. Due to the limited number of participants in each mutation subgroup, we assessed gray and white matter volume using mean w-maps instead of frequency w-maps.

Results

A subset of presymptomatic carriers harbors low mesial temporal lobe volumes

In total, the presymptomatic and symptomatic cohorts included 13 different *MAPT* mutation subtypes. For most neuropsychological measures, presymptomatic *MAPT* mutation carriers had no statistically significant differences compared to controls (Tables 2 and 3). The one exception was that presymptomatic carriers had a significantly lower but clinically negligible z-score of -0.39 on the Multilingual Naming Test (Table 2). With the three presymptomatic carriers with CDR® plus NACC FTLD global score of 0.5 excluded, results were similar with presymptomatic carriers largely showing no differences across measures, with the exception of the Multilingual Naming Test ($z = -0.39$, range $-1.68, 0.38$). Symptomatic carriers showed clinically significant impairments in verbal learning and memory as well as naming and semantic verbal fluency, and borderline to low average performance on most other measures, including attention, executive functioning, and visual recall, while Benson Figure Copy was relatively preserved (Table 2).

We found that symptomatic *MAPT* mutation carriers had severe bilateral mesial temporal atrophy as well as frontotemporal and insula atrophy and white matter involvement in the uncinate fasciculus, anterior corona radiata, corpus callosum, and inferior longitudinal fasciculus (Fig. 1; Fig. S1). Frequency w-maps revealed that each symptomatic carrier harbored prominent mesial temporal lobe atrophy and about sixty percent had involvement within frontotemporal white matter tracts (Fig. 1). Although the mean w-maps for presymptomatic carriers did not show any regions with low gray matter (defined as $w \leq -2$), we found that 20% of presymptomatic carriers had low mesial temporal lobe volumes and low white matter volume arose in approximately 10% (Fig. 1). When calculating the difference between each participant's mean left and right hemisphere w-score for gray or white matter, we found that at individual level, both symptomatic and presymptomatic participants had symmetric gray and white matter (maximum difference score $w = 0.78$ for a symptomatic carrier).

We repeated these analyses with presymptomatic carriers who had a CDR® plus NACC FTLD score of 0 only. Gray matter and white matter frequency w-maps showed similar results (data not shown), supporting that the three

Table 2. Neuropsychological testing of North American cohorts.

Test	Presymptomatic <i>MAPT</i>		Symptomatic <i>MAPT</i>		Omnibus Model F (df)
	Raw scores: mean(SD) or median[IQR]	z-scores: mean(SD) or median[IQR]	Raw scores: mean(SD) or median[IQR]	z-scores: mean(SD) or median[IQR]	
Global Cognition ⁴					
MoCA, total score	28 [26, 29]	0.11 [−0.96, 0.64]	22 [11, 25]	−3.10 [−8.97, −1.49]	11.24 (5, 79) ^{1,2}
Executive Functions/Processing Speed/Attention					
Trails A, correct lines per minute	80.15 (24.58)	0.24 (0.94)	37.58 (20.11)	−1.38 (0.77)	8.67 (5, 88) ^{1,2}
Trails B, correct lines per minute	34.42 (10.68)	0.33 (1.03)	16.65 (9.88)	−1.39 (0.96)	8.00 (5, 88) ^{1,2}
Digit span forward	9.03 (2.31)	0.16 (0.98)	6.50 (2.85)	−0.91 (1.21)	2.84 (5, 112) ^{1,2}
Digit span backward	8.00 (2.80)	0.21 (1.21)	5.24 (2.44)	−0.99 (1.05)	3.45 (5, 113) ^{1,2}
Semantic fluency, animals in 1 min	24.21 (6.34)	0.08 (1.17)	12.12 (8.42)	−2.14 (1.55)	12.79 (5, 113) ^{1,2}
Lexical fluency, words in 1 min	28.96 (7.04)	0.10 (0.91)	18.15 (12.73)	−1.29 (1.64)	7.10 (5, 81) ^{1,2}
Memory ⁴					
Total recall (California Verbal Learning Test, short form, four learning trials total)	31 [29, 32.5]	0.23 [−0.28, 0.61]	18 [15, 24]	−3.09 [−3.86, −1.56]	9.67 (5, 101) ^{1,2}
Delayed free recall (California Verbal Learning Test, short form, 10 min recall)	7 [6, 9]	−0.35 [−0.95, 0.85]	0 [0, 5]	−4.54 [−4.54, −1.54]	12.11 (5, 101) ^{1,2}
Benson figure 10 min recall, total score	14 [12, 16]	0.42 [−0.48, 1.31]	10 [4, 12]	−1.37 [−4.05, −0.48]	6.45 (5, 114) ^{1,2}
Language ⁴					
Multilingual Naming Test, total score	29.5 [27, 31]	−0.39 [−1.67, 0.38]	26.5 [22.5, 28.5]	−1.92 [−3.97, −0.90]	7.56 (5, 80) ^{1,3}
Visuospatial ⁴					
Benson figure copy, total score	16 [15, 16]	0.09 [−0.99, 0.09]	16 [15, 16]	0.09 [−0.99, 0.09]	0.60 (5, 114)

Means and standard deviations (SD) or medians and interquartile ranges (IQR) are reported.

¹Symptomatic cohort is significantly different from controls at $P < 0.05$.

²Presymptomatic cohort is significantly different from symptomatic cohort at $P < 0.05$.

³Presymptomatic cohort is significantly different from controls at $P < 0.05$.

⁴Z-scores estimated from reflected and log-transformed data were used to fit the regression models.

presymptomatic carriers with CDR® plus NACC FTLD scores of 0.5 were not driving the overall results.

Mesial temporal lobe and relationships with memory throughout the *MAPT* lifespan

To explore whether regions of low gray and white matter in presymptomatic *MAPT* mutation carriers might worsen with age, we created gray and white matter frequency w-maps for each age decade represented within our data. We found that approximately 20% of presymptomatic *MAPT* mutation carriers in their thirties showed low mesial temporal volumes (Fig. 2). When examining carriers in their forties and fifties, an increasing percentage of participants had low mesial temporal gray matter with each additional decade. The white matter frequency map (Fig. 1) suggested that low white matter volumes also arise in certain presymptomatic carriers, but in contrast to the gray matter maps, the percentage of participants with low white matter volumes did not clearly increase with each decade.

For symptomatic carriers with CDR® plus NACC FTLD global scores of 0.5, mesial and anterior temporal

lobe and anterior cingulate atrophy were most common, followed by insula and regions in dorsolateral prefrontal cortex (Fig. 3). With worsening symptom severity, atrophy within these regions grew increasingly more common and extensive. All carriers with a CDR® plus NACC FTLD global score of 1 had mesial temporal lobe atrophy and all carriers with a global score of 2 had regions of anterior cingulate and insular atrophy. By the time carriers reached a global score of 3, all showed widespread frontotemporal, insula, and uncinat fasciculus atrophy.

We examined relationships between memory measures and the hippocampus, selected as an *a priori* region of interest, and voxelwise gray matter maps. Verbal and spatial memory z-scores were correlated with hippocampal volumes across the whole *MAPT* cohort. Across symptomatic and presymptomatic carriers combined, lower scores in verbal recall (CVLT-II) were associated with lower left hippocampal volume ($\rho = 0.70$, $P < 0.001$) and lower scores in visual recall were associated with lower right hippocampal volume ($\rho = 0.44$, $P < 0.001$). To explore whether a *MAPT*-targeted gray matter region is also associated with memory measures, we created a

Table 3. Neuropsychological testing of Erasmus cohort.

Test	Presymptomatic <i>MAPT</i>		Omnibus Model F (df)
	Raw scores: mean(SD) or median[IQR]	z-scores: mean(SD) or median[IQR]	
Global Cognition ¹			
MMSE, total score	29.5 [29, 30]	0.28 [−0.28, 0.85]	3.88 (4, 37)
Executive Functions/Processing Speed/Attention			
Trails A, correct lines per minute	58.90 (21.66)	0.30 (1.08)	4.37 (4, 37)
Trails B, correct lines per minute	28.44 (11.99)	0.46 (1.29)	4.08 (4, 37)
Digit span forward	8.93 (2.56)	−0.04 (1.32)	1.79 (4, 37)
Digit span backward	6.50 (1.74)	0.05 (0.89)	2.04 (4, 37)
Semantic fluency, animals in 1 min	26.93 (6.17)	0.52 (1.22)	1.94 (4, 37)
Lexical fluency, total D, A, and T words	36.57 (14.94)	0.25 (1.30)	0.72 (4, 37)
Memory			
Total Recall (Rey Auditory Verbal Learning Test, total)	48.36 (8.95)	0.54 (0.96)	3.87 (4, 37)
Delayed Free Recall (Rey Auditory Verbal Learning Test)	9.79 (3.75)	0.34 (1.20)	2.34 (4, 37)
Language ¹			
Boston Naming Test, total score	54.5 [50, 58]	0.07 [−0.92, 0.85]	1.08 (4, 37)
Visuospatial ¹			
Clock drawing	12.5 [12, 13]	−0.05 [−0.39, 0.29]	1.16 (4, 37)

Means and standard deviations (SD) or medians and interquartile ranges (IQR) are reported.

The Erasmus presymptomatic cohort did not differ from controls for any measure.

¹Z-scores estimated from reflected and log-transformed data were used to fit the regression models.

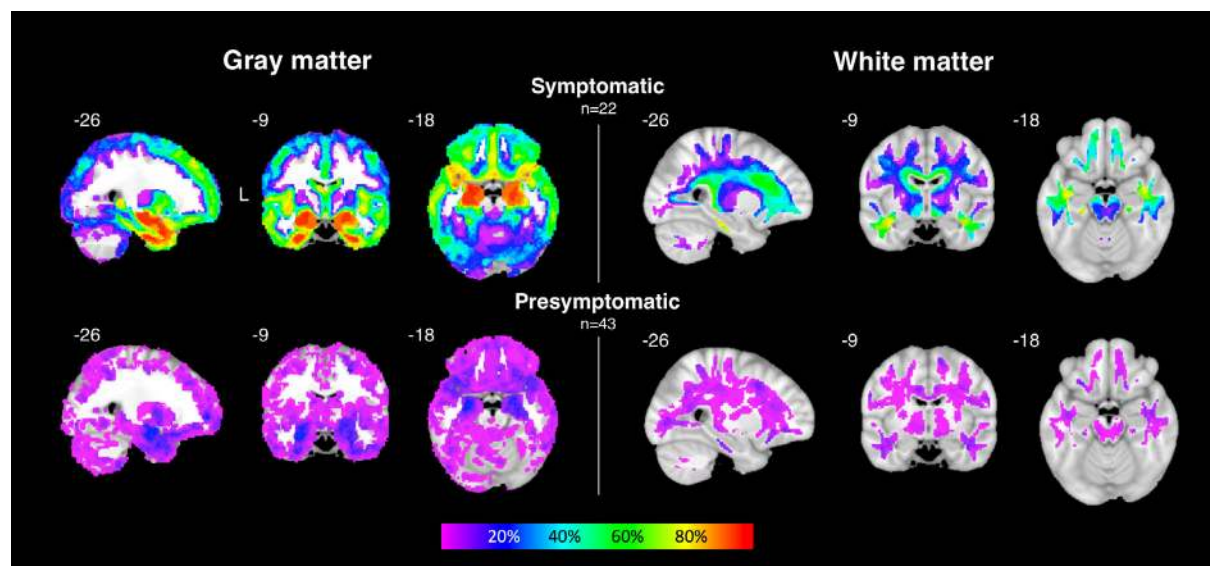


Figure 1. Gray and white matter frequency w-maps grouped by clinical stage. Frequency w-maps show the percentage of subjects within the group, ranging from 1% (magenta) to 100% of subjects (red), who have low gray or white matter volumes with $w \leq -2$ in a given voxel. Top row, left: All *MAPT* mutation carriers within the symptomatic group have anteromesial temporal atrophy. Top row, right: Symptomatic carriers have atrophy in the uncinate fasciculi, corpus callosum, and anterior corona radiata. Bottom row, left: Approximately 20% of presymptomatic *MAPT* mutation carriers show low gray matter volume in the mesial temporal lobes. Bottom row, right: Few carriers show low white matter volume before symptom onset. All maps are shown on the Montreal Neurological Institute template brain with the left side of the axial and coronal slices corresponding to the left side of the brain.

spherical region of interest centered on a left hippocampus voxel where carriers most frequently had low gray matter. We also created its contralateral homolog. Lower

verbal recall scores were associated with lower volume within this left hippocampal sphere ($\rho = 0.66$, $P < 0.001$), while lower scores in visual recall were

associated with lower right hippocampal sphere volume ($\rho = 0.50, <0.001$). Voxelwise, lower verbal recall was correlated with lower hippocampal volume bilaterally, while lower visual recall was associated with lower volume in a small clusters of the left hippocampus and other scattered voxels (Fig. 4). These three analyses (whole hippocampus, hippocampal sphere, voxelwise) were repeated with symptomatic and presymptomatic carrier subgroups and showed no statistically significant correlations between memory measures and gray matter.

We repeated each of these analyses by excluding the three presymptomatic carriers with the CDR® plus NACC FTLD score of 0.5 and results were unchanged.

Most *MAPT* mutation subtypes target frontotemporal cortex

When mean w-maps were calculated for each *MAPT* subtype, we found that most of the symptomatic *MAPT* mutation subtype groups (bvFTD-type, PSP/PD type, 4R-type) shared a consistent pattern of fronto-insulo-

temporal atrophy (Fig. 5). Of those groups, the bvFTD-type group showed the most severe gray and white matter frontotemporal atrophy, while the PSP/PD type group showed the most severe atrophy within the mesial temporal lobes (Fig. 5). One notable exception to the shared frontotemporal atrophy pattern, however, was the R406W mutation group, which typically results in an amnesic presentation. R406W carriers lacked the frontal gray and white matter atrophy that was characteristic of the other *MAPT* mutation subtypes, and instead only showed bilateral temporal and insular atrophy. Similar to the bvFTD-type and 4R-type mutations, the PSP/PD group showed frontotemporal atrophy, but additionally showed prominent midbrain atrophy. The presymptomatic carriers with PSP/PD-related mutations had low bilateral anterior cingulate, insula and mesial temporal volumes and were also the only presymptomatic group with voxels of low mid-brain volume, albeit in sparse regions. We found no differences in results when the three presymptomatic carriers with a CDR® plus NACC FTLD score of 0.5 were excluded.

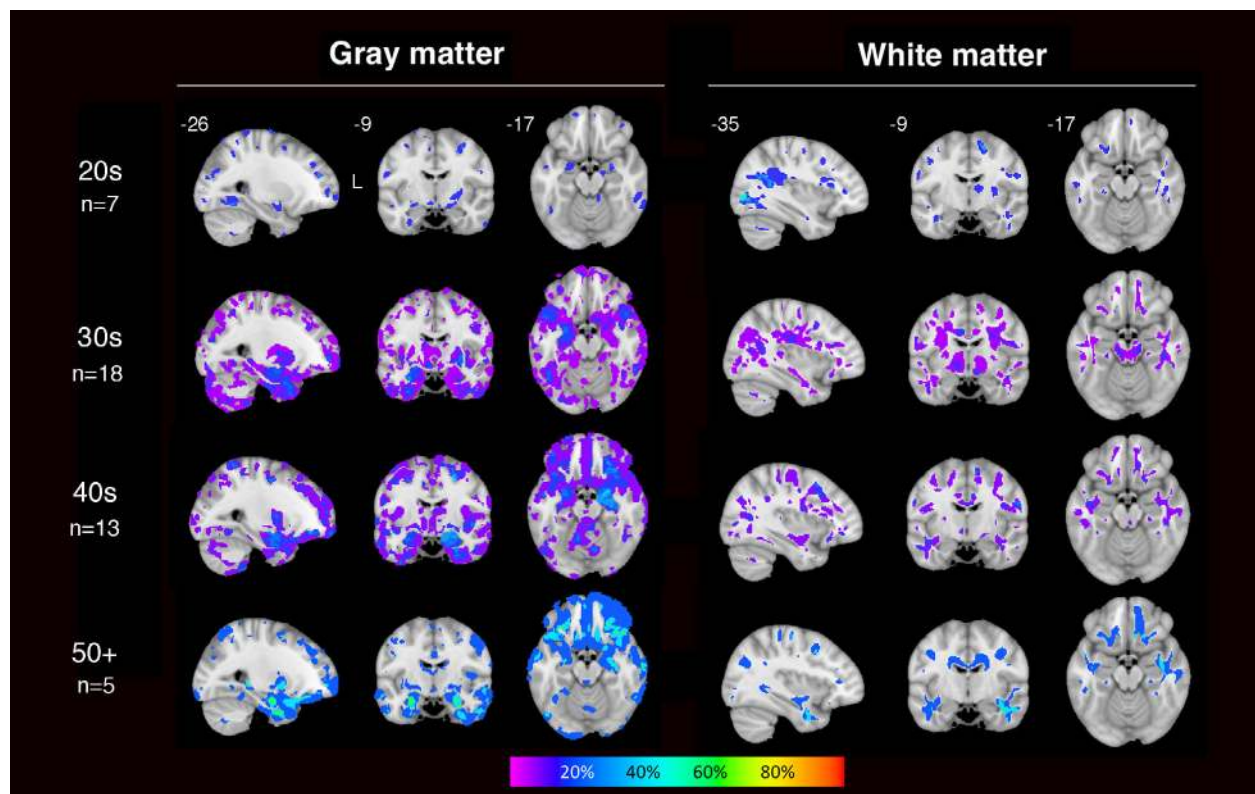


Figure 2. Gray and white matter frequency w-maps of presymptomatic carriers grouped by age decade. Gray matter (left) and white matter (right) frequency w-maps for presymptomatic carriers divided by age decade (rows). Color bar indicates the percentage of subjects within each age decade with low gray or white matter volumes of $w \leq -2$ in a given voxel. Low mesial temporal lobe volumes arise in about 20% of *MAPT* mutation carriers as early as their thirties. All maps are shown on the Montreal Neurological Institute template brain with the left side of the axial and coronal slices corresponding to the left side of the brain.

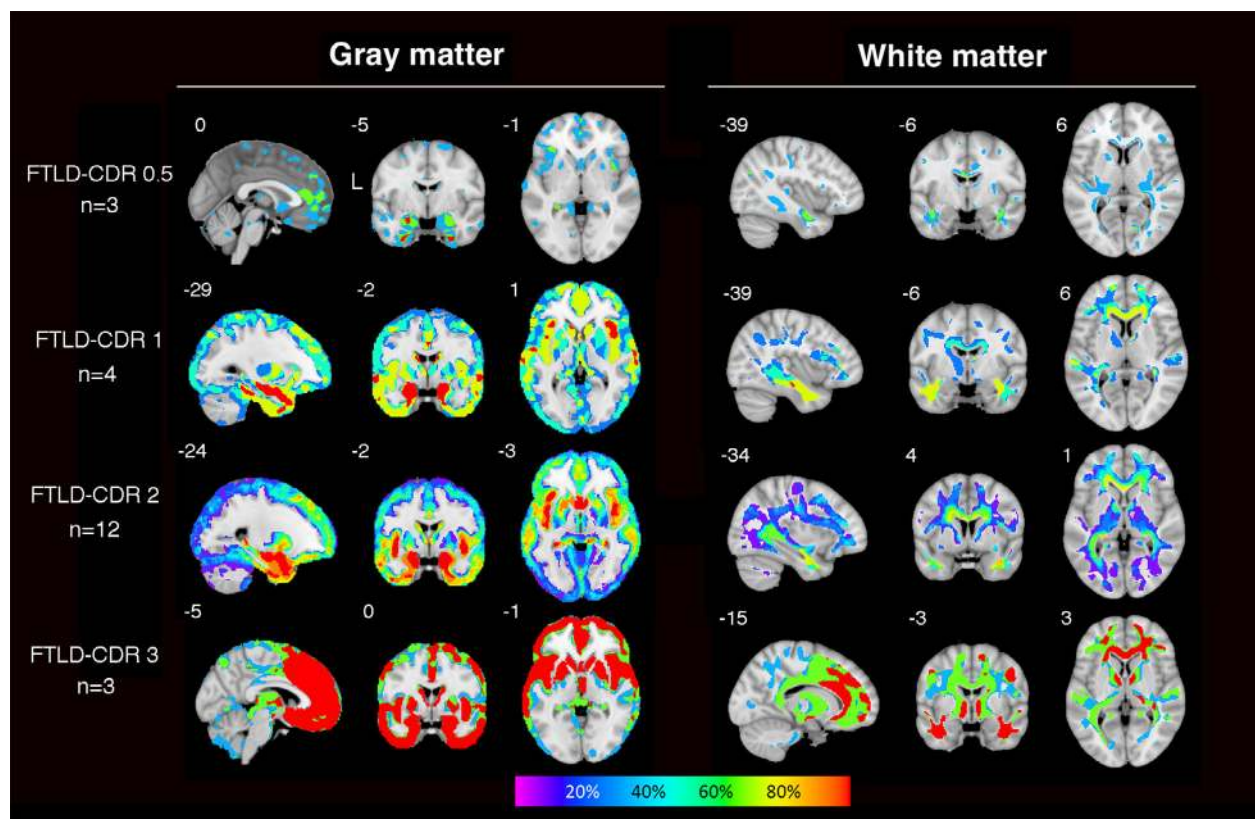


Figure 3. Gray and white matter frequency w-maps of symptomatic carriers grouped by symptom severity. Gray matter (left) and white matter (right) frequency w-maps for symptomatic carriers binned by symptom severity, as defined by the CDR® plus NACC FTLD global score (FTLD-CDR). Color bar indicates the percentage of subjects within each symptom severity category with gray or white matter atrophy of $w \leq -2$ in a given voxel. Mesial temporal lobe atrophy becomes ubiquitous in those with an FTLD-CDR score of 1. With worsening severity, atrophy within temporal and frontal lobes, insula and anterior cingulate are increasingly more common and extensive. All maps are shown on the Montreal Neurological Institute template brain with the left side of the axial and coronal slices corresponding to the left side of the brain.

Discussion

In this study, we took a comprehensive approach to identify individual-level variation in gray and white matter volume and their relationships with age or symptom severity across the *MAPT* continuum. We also identified relationships between memory performance and gray matter to explore whether specific *MAPT* mutation subtypes were associated with distinct atrophy patterns. We found that presymptomatic *MAPT* mutation carriers have low mesial temporal volumes that are topographically similar to the atrophy pattern seen in symptomatic carriers. Low mesial temporal lobe volumes arose in about 20% of the presymptomatic carriers during their thirties, and regions with low gray matter appeared more common in presymptomatic carriers with each increasing decade. Fewer than 10% of presymptomatic carriers had low white matter values in affected regions. For symptomatic carriers, mesial temporal cortex was ubiquitously atrophied in carriers with a CDR® plus NACC FTLD global score of 1 or greater, with

widespread atrophy in frontotemporal cortex in those with more advanced symptoms. In *MAPT* mutation carriers, poorer memory performance was associated with lower hippocampal volume. We found that atrophy in frontotemporal and insular cortex and the uncinate fasciculi, inferior longitudinal fasciculi, and corpus callosum were commonly observed across different *MAPT* mutations during the symptomatic phase, with the exception of the R406W mutation carriers who lacked the frontal atrophy characteristic of other *MAPT* mutation carriers.

A subset of presymptomatic carriers shows low mesial temporal volumes

As in previous studies, we found that frontotemporal cortex is targeted in symptomatic *MAPT* mutation carriers.^{2,3} Compared to patients with sporadic bvFTD and those with other FTLD mutations, prominent mesial temporal atrophy is more prevalent in *MAPT* mutation carriers,^{2,35,36} who feature correspondingly greater memory

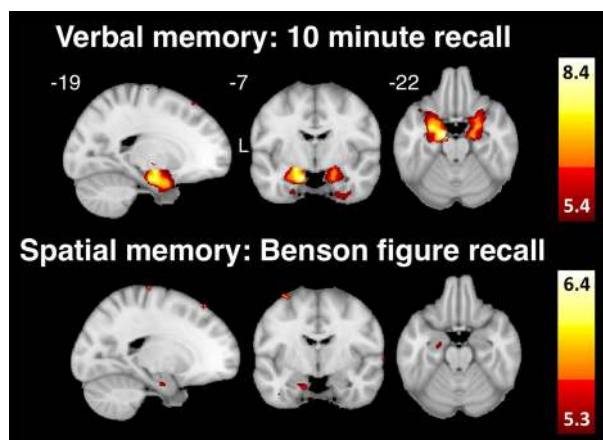


Figure 4. Voxelwise correlations between memory measures and gray matter. Maps show regions where verbal (top row) or spatial (bottom row) memory z-scores were significantly correlated with regions of low gray matter volume across all *MAPT* mutation carriers. Lower scores on a verbal memory measure was associated with low volume in bilateral hippocampi and inferior temporal regions. Lower scores on a spatial memory measure was associated with low gray matter in small scattered clusters including the left hippocampus, right middle frontal gyrus, frontal pole, and left dorsal parietal lobe. Maps were thresholded at $P < 0.05$, corrected for family-wise error. Color bars show t-value ranges. All maps are shown on the Montreal Neurological Institute template brain with the left side of the axial and coronal slices corresponding to the left side of the brain.

impairment.^{23,37} Although mean group w-maps did not identify regions of low matter in presymptomatic carriers, frequency w-maps revealed that 20% of this group had low mesial temporal volume. While early studies suggested that gray matter abnormalities were undetectable in presymptomatic *MAPT* mutation carriers,^{4,5} recent larger studies suggested that presymptomatic carriers have low hippocampal and amygdalar volumes.^{6,8,17,38} Several potential explanations may account for these varied results. First, low gray matter volumes during the presymptomatic phase are subtle and thus are likely to be detectable only with larger cohorts. Second, previous studies of presymptomatic carriers have performed group analyses, which may be insensitive to low brain volumes present in a minority of participants. By examining frequency maps, we were able to identify the subset of carriers with abnormally low gray and white matter volumes, thus circumventing this limitation. Third, the presymptomatic carriers in the present study and previous studies could have differences in the number of years until actual symptom onset. An individual's age of onset and mean familial age of onset are highly correlated, and perhaps more strongly correlated for *MAPT* mutation carriers compared to other FTD mutations.^{6,39} Although the mean age of the presymptomatic cohort in the present study is similar to previous studies,^{5,8,39} age and mean

familial age of onset remain imperfect methods for estimating the actual age of onset. Whether lower hippocampal gray matter volumes portend earlier conversion to the symptomatic phase remains an open question.

In contrast to sporadic bvFTD, memory impairment is a feature of bvFTD due to *MAPT* mutations.^{40,41} Indeed, we found that episodic memory, particularly verbal memory, was the most severely affected domain in symptomatic carriers. Despite memory and language impairments and lower than average executive performance, visuoconstructional performance was similar to controls. Our results showed that in all *MAPT* carriers combined, poorer memory performance was correlated with lower hippocampal volumes. Although hippocampal atrophy has been reported in *MAPT*,^{2,3,6,8,17,36,38} to our knowledge, previous studies have not directly correlated memory performance with hippocampal volume in *MAPT* mutation carriers. The hippocampus is well-established for its importance in episodic memory^{19,20} and our results support that this structure underlies the memory impairment in *MAPT*. Our subgroup analyses of symptomatic and presymptomatic carriers failed to identify significant correlations between memory measures and hippocampal volume. Smaller subgroup sample sizes, floor effects in the symptomatic carriers' memory scores, and the limited dynamic range of presymptomatic carriers' memory scores serve as possible explanations for these results.

Compared to gray matter, low white matter volume arose less frequently among presymptomatic carriers. One possibility is that gray matter decline precedes white matter decline during the presymptomatic phase. Consistent with this notion, a study of five presymptomatic *MAPT* mutation carriers followed over four years found that upon visual inspection, the extent of gray matter loss appeared more pronounced than white matter integrity loss.⁴² Although the present study showed that low white matter volumes as assessed by voxel-based morphometry were not prevalent in presymptomatic *MAPT*, diffusion tensor imaging studies have reported lower white matter tract integrity in presymptomatic *MAPT* compared to controls.^{7,43} Voxel-based morphometry may be less sensitive at detecting white matter differences compared to diffusion tensor imaging, thus future studies using multiple imaging modalities are needed.

Regions of low gray and white matter may reflect early neurodegeneration in presymptomatic carriers

Certain presymptomatic carriers in their thirties showed low mesial temporal volumes, consistent with a previous

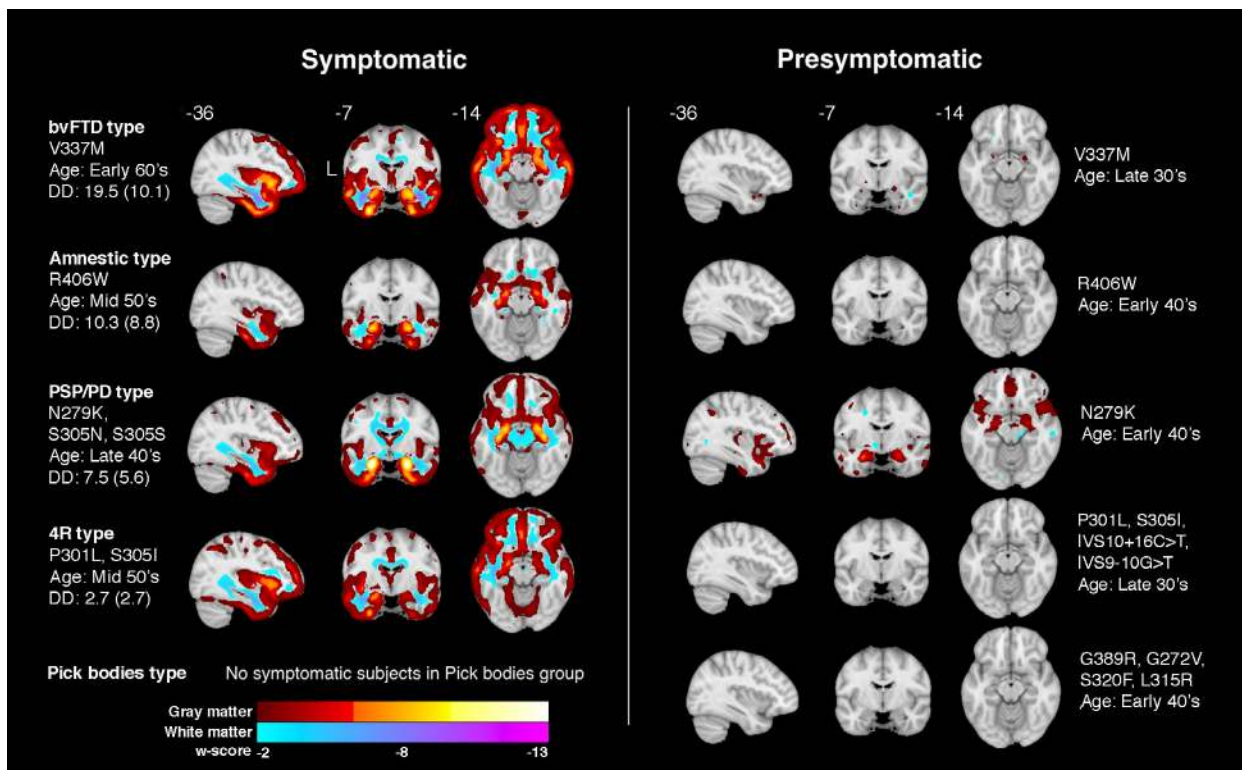


Figure 5. Atrophy patterns by *MAPT* mutation subtype —mean w-maps. Mean w-maps show the mean w-score in gray and white matter across all subjects grouped by clinical stage. Rows reflect five different mutation subtype groupings. Frontotemporal atrophy patterns are similar across mutation groups, except for the amnesic type R406W mutation group, which lacks frontal atrophy. Mutation subtypes associated with progressive supranuclear palsy or parkinsonism distinctly show midbrain atrophy for both the symptomatic and presymptomatic groups. The decade of the mean age for each group is indicated rather than the specific mean age in order to protect participant anonymity. Group maps are thresholded from $w \leq -13$ to -2 . All maps are shown on the Montreal Neurological Institute template brain with the left side of the axial and coronal slices corresponding to the left side of the brain. DD: disease duration.

study suggesting that gray matter trajectories indicate low hippocampal and amygdalar volumes arising 15 years before estimated symptom onset.⁶ While regions with low gray matter could in part reflect neurodevelopmental differences as has been suggested for the *C9orf72* repeat expansion,^{44,45} our data indicate that presymptomatic carriers more frequently had low volumes within canonical regions that are targeted in *MAPT* mutations with each age decade. This finding suggests that a subset of presymptomatic carriers may be undergoing incipient neurodegeneration, with more carriers following suit as symptom onset approaches. Interestingly, the frequency of low mesial temporal lobe volumes appeared to outpace other regions with increasing age, underscoring the notion that the mesial temporal lobe is targeted early in *MAPT* mutation carriers and becomes increasingly ubiquitous with age and throughout the symptomatic phase. A recent study of 14 presymptomatic *MAPT* mutation carriers studied over a median of 9 years revealed that the rate of temporal lobe gray matter decline outpaced the

rate of decline in the frontal and parietal cortices, suggesting that low temporal gray matter volumes in presymptomatic carriers may represent early neurodegeneration.⁴⁶

Most *MAPT* mutation subtypes converge on frontotemporal atrophy

Despite the different mechanisms of each mutation on tau protein biology and neuropathology, patients with different *MAPT* mutation subtypes converged on a highly similar pattern of frontal and anterior, mesial and lateral temporal atrophy with a corresponding predominance of bvFTD diagnoses.^{15,47,48} Another study found that six *MAPT* mutation subtypes shared anterior temporal gray matter atrophy.⁴¹ IVS10 + 16, IVS10 + 3, N279K, and S305N additionally showed mesial temporal atrophy, while P301L and V337M had lateral temporal regions targeted, with relative sparing of the mesial temporal lobe.⁴¹ In contrast, our V337M symptomatic carriers showed mesial temporal involvement. Both the present study and

previous studies have investigated small numbers of participants for each mutation subtype, such that clinical heterogeneity may influence results.

Two notable exceptions arose when studying *MAPT* mutation subtypes. R406W is the only known *MAPT* mutation that causes an amnesic syndrome rather than a behavioral syndrome,^{22,23} and it typically causes mesial temporal atrophy while sparing the frontal lobes relative to other *MAPT* mutations.^{22,23,49,50} We found that R406W carriers exclusively showed mesial and lateral temporal atrophy, but lacked frontal atrophy, which may explain why these carriers develop an amnesic rather than a bvFTD syndrome. Among the *MAPT* mutations we studied, N279K, S305N, and S305S cause PSP and parkinsonism. Interestingly, this group was the only *MAPT* group which had midbrain atrophy, and midbrain atrophy has been associated with patients with PSP.⁵¹ An important caveat to our findings is that variability in age and disease duration within the subtype groups may be contributing to differences in atrophy because the participant numbers are limited for each group. Remarkably, the average disease duration ranged from 2.7 (\pm 2.7) years for the 4R-type mutation group to 19.5 (\pm 10.1) years for V337M carriers, yet despite this wide range, the magnitude of atrophy among the four mutation groups was similar. This long disease duration and relatively old average age of onset suggests that V337M might have a more indolent, protracted disease course compared to the other mutations.

Limitations

This study examined one of the largest *MAPT* cohorts to date, but sample sizes were still small within most mutation subtypes and larger cohorts are needed to study individual *MAPT* mutations. To maximize power, we combined different mutation subtypes based on clinical or neuropathological similarity. Although we examined relationships of gray and white matter with age, this study had a cross-sectional design and longitudinal analyses are needed to map disease trajectories. The extent to which focal regions with low gray and white matter in presymptomatic mutation carriers may be due to neurodevelopmental differences versus early neurodegeneration remains unknown. Yet, the present study and current literature support the notion that low gray and white matter volumes in presymptomatic *MAPT* mutation carriers represent early neurodegeneration. Longitudinal studies will clarify these questions by mapping trajectories in *MAPT* mutation carriers from early life through the symptomatic phase.

Acknowledgements

The manuscript has been reviewed by the Publications Committee of LEFFTDS & ARTFL for scientific content.

The authors thank the ARTFL & LEFFTDS consortium, and the National Centralized Repository for Alzheimer's Disease and Related Dementias. The authors acknowledge the invaluable contributions of the participants at the Memory and Aging Center, Erasmus University Rotterdam, and ARTFL & LEFFTDS, as well as the assistance of the support staff at each of the participating sites.

Conflicts of Interest

SAC, TMF, LCJ, JD, SS, LZ, VES, JSY, WWS, JMP, DHG, HWH, LKF, DEB, MG, YMB, JCF, TF, RHG, DJI, AMK, JHK, WAK, MIL, MFM, AYP, RR, EMR, MCT, NAT, AV, SW, BW, JCVS, and SEL had no disclosures. AMS received research support from the Larry H. Hillblom foundation and support from the NIH. HJR received research support from Biogen Pharmaceuticals, has consulting agreements with Wave Neuroscience and Ionis Pharmaceuticals, and receives research support from the NIH. BFB served as an investigator for clinical trials sponsored by GE Healthcare and Axovant. He received royalties from the publication of a book entitled Behavioral Neurology of Dementia (Cambridge Medicine, 2009, 2017). He served on the Scientific Advisory Board of the Tau Consortium. He received research support from the NIH, the Mayo Clinic Dorothy and Harry T. Mangurian Jr. Lewy Body Dementia Program and the Little Family Foundation. ALB received research support from the NIH, the Tau Research Consortium, the Association for Frontotemporal Degeneration, Bluefield Project to Cure Frontotemporal Dementia, Corticobasal Degeneration Solutions, the Alzheimer's Drug Discovery Foundation, and the Alzheimer's Association. He served as a consultant for Aeton, Abbvie, Alector, Amgen, Arkuda, Ionis, Iperian, Janssen, Merck, Novartis, Samumed, Toyama and UCB, and received research support from Avid, Biogen, BMS, C2N, Cortice, Eli Lilly, Forum, Genentech, Janssen, Novartis, Pfizer, Roche, and TauRx. GC, BCD, KF, JAF, EDH, BLM, AWT received research support from the NIH. HHF reported grants from Toyama Pharmaceuticals, Biohaven Pharmaceuticals, Annovis Bio (QR Pharma) and Vivoryon (Probiodrugs). He also reported service agreements through UCSD for consulting with Eisai, Merck, Tau RX, Samus, Arkuda, Samumed, Axon Neurosciences, Roche/Genentech Pharmaceuticals for DMC and DSMB activities; Tau Consortium for Scientific Advisory Board. He reported travel expenses from Vivoryon, Axon Neurosciences and Alion Pharmaceuticals and speaker fees to UCSD from World Events Forum, Optum Health, and Medscape. NG had participated or is currently participating in clinical trials of antidementia drugs sponsored by the following companies: Bristol Myers

Squibb, Eli Lilly/Avid Radiopharmaceuticals, Janssen Immunotherapy, Novartis, Pfizer, Wyeth, SNIFF (The Study of Nasal Insulin to Fight Forgetfulness) study, and A4 (The Anti-Amyloid Treatment in Asymptomatic Alzheimer's Disease) trial. She received research support from Tau Consortium and Association for Frontotemporal Dementia and is funded by the NIH. NRGR received royalties from UpToDate and had participated in multicenter therapy studies sponsored by Biogen, TauRx, AbbVie, Novartis, and Lilly. He received research support from the NIH. GYRH had served as an investigator for clinical trials sponsored by AstraZeneca, Eli Lilly, and Roche/Genentech. He received research support from the Canadian Institutes of Health Research and the Alzheimer Society of British Columbia. KK served on the Data Safety Monitoring Board for Takeda Global Research & Development Center, Inc.; data monitoring boards of Pfizer and Janssen Alzheimer Immunotherapy; research support from the Avid Radiopharmaceuticals, Eli Lilly, the Alzheimer's Drug Discovery Foundation, and the NIH. DIK served as a consultant to Axovant, Abbvie, Janssen Research and Development, and Takeda. He served on the advisory board of Grifols, and received research support from Axovant, Janssen Research and Development, Navidea Biopharmaceuticals, and Acadia. DSK served on the DSMB of the DIAN-TU study, is a site PI for clinical trials sponsored by Biogen, Lilly and the University of Southern California, and is funded by the NIH. JK had provided expert witness testimony for Teva Pharmaceuticals in *Forest Laboratories Inc. et al. v. Teva Pharmaceuticals USA, Inc.*, Case Nos. 1:14-cv-00121 and 1:14-cv-00686 (D. Del. filed Jan. 31, 2014 and May 30, 2014) regarding the drug Memantine; for *Apotex/HEC/Ezra in Novartis AG et al. v. Apotex Inc.*, No. 1:15-cv-975 (D. Del. filed Oct. 26, 2015, regarding the drug Fingolimod. He had also given testimony on behalf of Puma Biotechnology in *Hsingching Hsu et al., vs. Puma Biotechnology, INC., et al.* 2018 regarding the drug neratinib. He received research support from the NIH. IL received research support from the NIH, Parkinson Study Group, Parkinson Foundation, Michael J Fox Foundation, AVID Pharmaceuticals, C2N Diagnostics/Abbvie, and Bristol-Myers Squibb. She was a member of the Biogen and Bristol-Myers Squibb Advisory Boards, Biotie/Parkinson Study Group Medical Advisory Board, and consultant for Toyama Pharmaceuticals. She received salary from the University of California San Diego and as Editor in *Frontiers in Neurology*. IRAM received research funding from the Canadian Institutes of Health Research. S.M.M. served as an investigator for clinical trials sponsored by AbbVie, Allon Therapeutics, Biogen, Bristol-Myers Squibb, C2N Diagnostics, Eisai Inc., Eli Lilly and Co., Genentech, Janssen Pharmaceuticals, Medivation, Merck, Navidea

Biopharmaceuticals, Novartis, Pfizer, and TauRx Therapeutics. He received research support from the NIH. CUO received research funding from the NIH, the CIHR, and Biogen, Inc. He was also supported by the Jane Tanner Black Fund for Young-Onset Dementias, the Nancy H. Hall Fund for Geriatric Psychiatry, and the gift from Joseph Trovato. EDR received research support from the NIH, Bluefield Project to Cure Frontotemporal Dementia, Alzheimer's Association, BrightFocus Foundation, Biogen, Alector, and owns intellectual property related to tau. ZKW was supported by the NIH, Mayo Clinic Center for Regenerative Medicine, the gift from Carl Edward Bolch, Jr., and Susan Bass Bolch, the Sol Goldman Charitable Trust, and Donald G. and Jodi P. Heeringa. He has also received grant funding support from Allergan, Inc. (educational grant), and Abbvie (medication trials).

Author Contributions

SAC, SEL, SS, and WWS contributed to the conception and design of the study. SAC and SEL contributed to drafting the manuscript. SAC, TMF, AMS, JD, LZ, and SEL contributed to data analysis. AMS, LCJ, SS, VES, JSY, WWS, JMP, HJR, BFB, ALB, HWH, LKF, DEB, MG, GC, BC, YMB, KF, HHF, JAF, JCF, TF, RHG, NG, NRGR, GYRH, EDH, DJI, KK, DIK, AMK, DSK, JK, JHK, WAK, MIL, IL, IRAM, MFM, BLM, CUO, AYP, RR, EMR, EDR, MCT, NAT, AWT, AV, SW, BW, ZKW, JCVS, and SEL contributed to data acquisition.

References

- Ghetti B, Wszolek ZK, Boeve BF, et al. Frontotemporal Dementia and Parkinsonism Linked to Chromosome 17. Neurodegeneration: The Molecular Pathology of Dementia and Movement Disorders. Ltd: John Wiley & Sons, 2011:110–134. <https://doi.org/10.1002/9781444341256.ch14>.
- Rohrer JD, Ridgway GR, Modat M, et al. Distinct profiles of brain atrophy in frontotemporal lobar degeneration caused by progranulin and tau mutations. *NeuroImage* 2010;53:1070–1076. <https://doi.org/10.1016/j.neuroimage.2009.12.088>.
- Whitwell JL, Jack CR, Boeve BF, et al. Voxel-based morphometry patterns of atrophy in FTLTD with mutations in MAPT or PGRN. *Neurology* 2009;72:813–820. <https://doi.org/10.1212/01.wnl.0000343851.46573.67>.
- Dopper EGP, Rombouts SAR, Jiskoot LC, et al. Structural and functional brain connectivity in presymptomatic familial frontotemporal dementia. *Neurology* 2013;80:814–823. <https://doi.org/10.1212/WNL.0b013e31828407bc>.
- Whitwell JL, Josephs KA, Avula R, et al. Altered functional connectivity in asymptomatic MAPT subjects. *Neurology*

- 2011;77:866–874. <https://doi.org/10.1212/WNL.0b013e31822c61f2>.
6. Rohrer JD, Nicholas JM, Cash DM, et al. Presymptomatic cognitive and neuroanatomical changes in genetic frontotemporal dementia in the Genetic Frontotemporal dementia Initiative (GENFI) study: a cross-sectional analysis. *Lancet Neurol* 2015;14:253–262. [https://doi.org/10.1016/S1474-4422\(14\)70324-2](https://doi.org/10.1016/S1474-4422(14)70324-2).
 7. Jiskoot LC, Bocchetta M, Nicholas JM, et al. Presymptomatic white matter integrity loss in familial frontotemporal dementia in the GENFI cohort: A cross-sectional diffusion tensor imaging study. *Ann Clin Transl Neurol* 2018;5:1025–1036. <https://doi.org/10.1002/acn3.601>.
 8. Cash DM, Bocchetta M, Thomas DL, et al. Patterns of gray matter atrophy in genetic frontotemporal dementia: results from the GENFI study. *Neurobiol Aging*. 2018;62:191–196. <https://doi.org/10.1016/j.neurobiolaging.2017.10.008>.
 9. Boeve B, Bove J, Brannelly P, et al. The longitudinal evaluation of familial frontotemporal dementia subjects protocol: Framework and methodology. *Alzheimers Dement J Alzheimers Assoc*. 2020;16:22–36. <https://doi.org/10.1016/j.jalz.2019.06.4947>.
 10. Nasreddine ZS, Phillips NA, Bédirian V, et al. The Montreal Cognitive Assessment, MoCA: a brief screening tool for mild cognitive impairment. *J Am Geriatr Soc*. 2005;53:695–699. <https://doi.org/10.1111/j.1532-5415.2005.53221.x>.
 11. Trzepacz PT, Hochstetler H, Wang S, et al. Alzheimer's Disease Neuroimaging Initiative. Relationship between the Montreal Cognitive Assessment and Mini-mental State Examination for assessment of mild cognitive impairment in older adults. *BMC Geriatr*. 2015;15(1); <https://doi.org/10.1186/s12877-015-0103-3>.
 12. Knopman DS, Kramer JH, Boeve BF, et al. Development of methodology for conducting clinical trials in frontotemporal lobar degeneration. *Brain* 2008;131(11):2957–2968. <https://doi.org/10.1093/brain/awn234>.
 13. Kramer JH. Distinctive neuropsychological patterns in frontotemporal dementia, semantic dementia, and Alzheimer disease. *Cogn Behav Neurol Off J Soc Behav Cogn Neurol* 2003;16:211–218.
 14. Weintraub S, Besser L, Dodge H, et al. Version 3 of the Alzheimer Disease Centers' Neuropsychological test battery in the uniform data set (UDS). *Alzheimer Dis Assoc Disord* 2018;32:10–17. <https://doi.org/10.1097/WAD.0000000000000223>.
 15. Hutton M, Lendon CL, Rizzu P, et al. Association of missense and 5'-splice-site mutations in *tau* with the inherited dementia FTDP-17. *Nature* 1998;393:702–705. <https://doi.org/10.1038/31508>.
 16. La Joie R, Perrotin A, Barré L, et al. Region-specific hierarchy between atrophy, hypometabolism, and β -amyloid (A β) load in Alzheimer's disease dementia. *J Neurosci Off J Soc Neurosci* 2012;32:16265–16273. <https://doi.org/10.1523/JNEUROSCI.2170-12.2012>.
 17. Olney NT, Ong E, Goh S-YM, et al. Clinical and volumetric changes with increasing functional impairment in familial frontotemporal lobar degeneration. *Alzheimers Dement J Alzheimers Assoc* 2020;16:49–59. <https://doi.org/10.1016/j.jalz.2019.08.196>.
 18. Tzourio-Mazoyer N, Landeau B, Papathanassiou D, et al. Automated Anatomical labeling of activations in SPM using a macroscopic anatomical parcellation of the MNI MRI single-subject brain. *NeuroImage* 2002;15:273–289. <https://doi.org/10.1006/nimg.2001.0978>.
 19. Milner B. Interhemispheric differences in the localization of psychological processes in man. *Br Med Bull* 1971;27:272–277. <https://doi.org/10.1093/oxfordjournals.bmb.a070866>.
 20. Maguire EA, Frackowiak RSJ, Frith CD. Recalling Routes around London: Activation of the Right Hippocampus in Taxi Drivers. *J Neurosci* 1997;17:7103–7110. <https://doi.org/10.1523/JNEUROSCI.17-18-07103.1997>.
 21. Poorkaj P, Bird TD, Wijsman E, et al. Tau is a candidate gene for chromosome 17 frontotemporal dementia. *Ann Neurol* 1998;43:815–825. <https://doi.org/10.1002/ana.410430617>.
 22. Reed LA, Schelper RL, Solodkin A, et al. Autosomal dominant dementia with widespread neurofibrillary tangles. *Ann Neurol* 1997;42:564–572. <https://doi.org/10.1002/ana.410420406>.
 23. Ygland E, van Westen D, Englund E, et al. Slowly progressive dementia caused by MAPT R406W mutations: longitudinal report on a new kindred and systematic review. *Alzheimers Res Ther* 2018;10:2. <https://doi.org/10.1186/s13195-017-0330-2>.
 24. Delisle MB, Murrell JR, Richardson R, et al. A mutation at codon 279 (N279K) in exon 10 of the Tau gene causes a tauopathy with dementia and supranuclear palsy. *Acta Neuropathol (Berl)* 1999;98:62–77.
 25. Hasegawa M, Smith MJ, Iijima M, et al. FTDP-17 mutations N279K and S305N in tau produce increased splicing of exon 10. *FEBS Lett* 1999;443:93–96. [https://doi.org/10.1016/S0014-5793\(98\)01696-2](https://doi.org/10.1016/S0014-5793(98)01696-2).
 26. Iijima M, Tabira T, Poorkaj P, et al. A distinct familial presenile dementia with a novel missense mutation in the tau gene. *NeuroReport* 1999;10:497–501.
 27. Skoglund L, Viitanen M, Kalimo H, et al. The tau S305S mutation causes frontotemporal dementia with parkinsonism. *Eur J Neurol* 2008;15:156–161. <https://doi.org/10.1111/j.1468-1331.2007.02017.x>.
 28. Stanford PM, Halliday GM, Brooks WS, et al. Progressive supranuclear palsy pathology caused by a novel silent mutation in exon 10 of the tau gene: expansion of the disease phenotype caused by tau gene mutations. *Brain J Neurol*. 2000;123(Pt 5):880–893.
 29. Kovacs GG, Pittman A, Revesz T, et al. MAPT S305I mutation: implications for argyrophilic grain disease. *Acta*

- Neuropathol (Berl) 2008;116:103–118. <https://doi.org/10.1007/s00401-007-0322-6>.
30. Malkani R, D'Souza I, Gwinn-Hardy K, et al. A *MAPT* mutation in a regulatory element upstream of exon 10 causes frontotemporal dementia. *Neurobiol Dis* 2006;22:401–403. <https://doi.org/10.1016/j.nbd.2005.12.001>.
 31. Murrell JR, Spillantini MG, Zolo P, et al. Tau gene mutation G389R causes a tauopathy with abundant pick body-like inclusions and axonal deposits. *J Neuropathol Exp Neurol* 1999;58:1207–1226.
 32. Bronner IF, ter Meulen BC, Azmani A, et al. Hereditary Pick's disease with the G272V tau mutation shows predominant three-repeat tau pathology. *Brain* 2005;128:2645–2653. <https://doi.org/10.1093/brain/awh591>.
 33. Rosso SM, Herpen EV, Deelen W, et al. A novel tau mutation, S320F, causes a tauopathy with inclusions similar to those in Pick's disease. *Ann Neurol* 2002;51:373–376. <https://doi.org/10.1002/ana.10140>.
 34. Herpen EV, Rosso SM, Serverijnen L-A, et al. Variable phenotypic expression and extensive tau pathology in two families with the novel tau mutation L315R. *Ann Neurol* 2003;54:573–581. <https://doi.org/10.1002/ana.10721>.
 35. Whitwell JL, Przybelski SA, Weigand SD, et al. Distinct anatomical subtypes of the behavioural variant of frontotemporal dementia: a cluster analysis study. *Brain* 2009;132:2932–2946. <https://doi.org/10.1093/brain/awp232>.
 36. Whitwell JL, Weigand SD, Boeve BF, et al. Neuroimaging signatures of frontotemporal dementia genetics: C9ORF72, tau, progranulin and sporadics. *Brain J Neurol* 2012;135(Pt 3):794–806. <https://doi.org/10.1093/brain/aww001>.
 37. Rascovsky K, Hodges JR, Knopman D, et al. Sensitivity of revised diagnostic criteria for the behavioural variant of frontotemporal dementia. *Brain* 2011;134:2456–2477. <https://doi.org/10.1093/brain/awr179>.
 38. Domínguez-Vivero C, Wu L, Lee S, et al. Structural brain changes in pre-clinical FTD *MAPT* mutation carriers. *J Alzheimers Dis JAD* 2020;75:595–606. <https://doi.org/10.3233/JAD-190820>.
 39. Moore KM, Nicholas J, Grossman M, et al. Age at symptom onset and death and disease duration in genetic frontotemporal dementia: an international retrospective cohort study. *Lancet Neurol* 2020;19:145–156. [https://doi.org/10.1016/S1474-4422\(19\)30394-1](https://doi.org/10.1016/S1474-4422(19)30394-1).
 40. Swieten JV, Spillantini MG. Hereditary frontotemporal dementia caused by tau gene mutations. *Brain Pathol* 2007;17(1):63–73. <https://doi.org/10.1111/j.1750-3639.2007.00052.x>.
 41. Whitwell JL, Jack CR, Boeve BF, et al. Atrophy patterns in IVS10+16, IVS10+3, N279K, S305N, P301L, and V337M *MAPT* mutations. *Neurology* 2009;73:1058–1065. <https://doi.org/10.1212/WNL.0b013e3181b9c8b9>.
 42. Jiskoot LC, Panman JL, Meeter LH, et al. Longitudinal multimodal MRI as prognostic and diagnostic biomarker in presymptomatic familial frontotemporal dementia. *Brain* 2019;142:193–208. <https://doi.org/10.1093/brain/awy288>.
 43. Chen Q, Boeve BF, Schwarz CG, et al. Tracking white matter degeneration in asymptomatic and symptomatic *MAPT* mutation carriers. *Neurobiol Aging* 2019;83:54–62. <https://doi.org/10.1016/j.neurobiolaging.2019.08.011>.
 44. Bertrand A, Wen J, Rinaldi D, et al. Early cognitive, structural, and microstructural changes in Presymptomatic C9orf72 carriers younger than 40 years. *JAMA Neurol* 2018;75:236–245. <https://doi.org/10.1001/jamaneurol.2017.4266>.
 45. Lee SE, Sias AC, Mandelli ML, et al. Network degeneration and dysfunction in presymptomatic C9ORF72 expansion carriers. *NeuroImage Clin* 2017;14:286–297. <https://doi.org/10.1016/j.nicl.2016.12.006>.
 46. Chen Q, Boeve BF, Senjem M, et al. Rates of lobar atrophy in asymptomatic *MAPT* mutation carriers. *Alzheimers Dement Transl Res Clin Interv* 2019;5:338–346. <https://doi.org/10.1016/j.trci.2019.05.010>.
 47. Ghetti B, Oblak AL, Boeve BF, et al. Invited review: Frontotemporal dementia caused by microtubule-associated protein tau gene (*MAPT*) mutations: a chameleon for neuropathology and neuroimaging. *Neuropathol Appl Neurobiol* 2015;41:24–46. <https://doi.org/10.1111/nan.12213>.
 48. Spillantini MG, Crowther RA, Kamphorst W, et al. Tau pathology in two Dutch families with mutations in the microtubule-binding region of tau. *Am J Pathol* 1998;153:1359–1363. [https://doi.org/10.1016/S0002-9440\(10\)65721-5](https://doi.org/10.1016/S0002-9440(10)65721-5).
 49. Ikeuchi T, Imamura T, Kawase Y, et al. Evidence for a common founder and clinical characteristics of Japanese families with the *MAPT* R406W mutation. *Dement Geriatr Cogn Disord EXTRA*. 2011;1:267–275. <https://doi.org/10.1159/000331243>.
 50. Jones DT, Knopman DS, Graff-Radford J, et al. In vivo 18F-AV-1451 tau PET signal in *MAPT* mutation carriers varies by expected tau isoforms. *Neurology* 2018;90:e947–e954. <https://doi.org/10.1212/WNL.0000000000005117>.
 51. Massey LA, Jäger HR, Paviour DC, et al. The midbrain to pons ratio. *Neurology* 2013;80:1856–1861. <https://doi.org/10.1212/WNL.0b013e318292a2d2>.

Supporting Information

Additional supporting information may be found online in the Supporting Information section at the end of the article.

Figure S1. Gray and white matter mean w-maps of symptomatic carriers. Maps show the mean w-score of gray and white matter across the symptomatic carriers.

Symptomatic carriers have atrophy in frontotemporal cortex, insula, uncinate fasciculus, anterior corona radiata, corpus callosum, and inferior longitudinal fasciculus. Maps are thresholded from $w \leq -13$ to -2 . All maps are

shown on the Montreal Neurological Institute template brain with the left side of the axial and coronal slices corresponding to the left side of the brain.

Table S1. Participants by Site